Draft version December 21, 2024
Typeset using LaTeX **twocolumn** style in AASTeX631

Photometric Analysis of Bright Nebular Emission High-Redshift (z∼5.9) Galaxy

Sally[1] and Fred[1]

[1] *Columbia University Department of Astronomy, Pupin Hall, New York, NY, 10027, USA*

1. INTRODUCTION/MOTIVATION

Our early theories of how the first stars formed and the environment in and evolution of the first galaxies are now being tested. The James Webb Space Telescope (JWST), having been commissioned for more than a couple of years now, has ushered a new era of galaxy formation and evolution research at high redshift ($z \gtrsim 6$), giving a view of a strikingly active early universe, characterized by high star formation rates and massive black hole (BH) growth (see e.g., Adamo et al. 2024; Lupi et al. 2024).

In this paper, we focus on observation of JADES-GS+53.12175 -27.7976. Also known as GS-NDG-9422/ GS9422, this object is a high-redshift galaxy with photometry acquired as part of the GTO JWST Advanced Deep Extragalactic Survey (JADES) as described in (Eisenstein et al. 2023; Bunker et al. 2024). This object is of notable interest; e.g., Cameron et al. (2024) found strong spectral discontinuity near $\lambda_{\rm rest} = 3645$ Å, interpreted as strong emission from nebular gas. This would indicate the gas from this galaxy is extremely bright and possibly hot. The source heating this gas could come from two origins: massive stars or a combination of emissions from Active Galactic Nuclei (AGNs) and stars. Cameron et al. (2024) claim that the high nebular emission can be a result of a top-heavy IMF, causing the galaxy to consist mostly of star clusters with high-mass and low-metallicity stars. They claim the emission could not come from AGNs or an X-ray binary, as the source is observed to have weak HeII emission lines. However, Scholtz et al. (2023) believes the source's emission could originate from accretions around an AGN due to the measured HeII line ratios. This is further supported by Li et al. (2024), which used a model with both a central AGN and normal IMF-shaped stellar population powering the ionizing radiation in the galaxy and found it was consistent with observations.

In this work, we will investigate the stellar population and star formation history of GS9422. We do this to better understand the results found from both interpretations from all papers, it would be interesting to examine the photometric and spectroscopic data ourselves and possibly measure the stellar population of the source. This will be done by examining the photometry of the source taken by JWST and fitting models and extracting parameters on the source. We will see whether our analysis supports a top-heavy IMF model or an AGN+stars model interpretation.

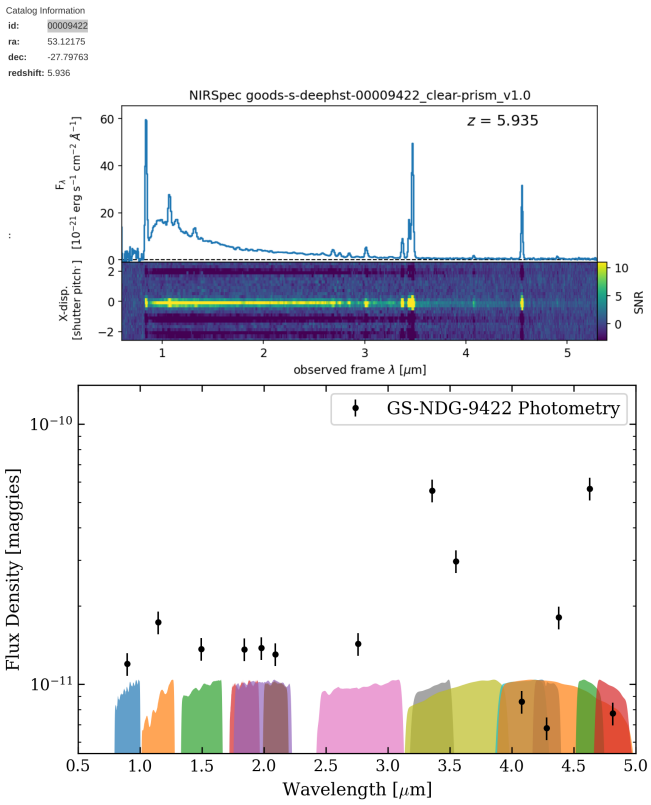

Figure 1. Top panel shows the spectrum for the object in question as viewed in the JADES fits viewer. JWST photometry data acquired for GS942 are shown as points with errror bars. The photometric values are roughyl centered in wavelength for all relevant JWST filters including F115W, F150W, F182M, F200W, F210M, F277W, F335M, F356W, F410M, F430M, F444W, F460M, and F480M.

2. DATA

Photometric Observations for GS9422 were obtained from the JWST Advanced Deep Extragalactic Survey

(JADES) program (Eisenstein et al. 2023; Rieke et al. 2023) Second Data Release. The program surveyed a massive 100 square arc minutes region, obtaining data with NIRCam, NIRSpec, and MIRI, taking photometric measurements for over 45,000 sources and spectra for over 2000 sources. Photometric measurements were combined with the JWST Extragalactic Medium-band Survey (JEMS) dataset (Williams et al. 2023).

The photometry was compiled into a catalog, and the source's RA and DEC were used to identify its ID in all photometric catalogs. For our photometric fitting later, we need to have photometry measurements in units of maggies. Our photometry measurements are given in units of nano-Janskies (nJy). We first convert these to Jansky and then into AB-magnitudes:

$$m_{\rm AB} = \frac{-2.5\log_{10}(\text{data[Jy]})}{3631\ \text{Jy}} \tag{1}$$

The AB-magnitudes were then converted into magnitudes in units of maggies by the following relation:

$$m_{\rm maggies} = 10^{-0.4 m_{\rm AB}}. \tag{2}$$

3. ANALYSIS

3.1. *Prospector Photometry*

We use the package `PROSPECTOR` (Johnson et al. 2021) to fit our photometric data. Our initial model does not include any nebular emission. Some parameters we changed when we built the model include: observed signal to noise (snr) = 10 and luminosity distance (ldist) = 5.832e+04 Mpc (found from converting the redshift of the source to a distance). Figure 1 shows the photometry of our dataset and the transmission filters overplotted. We can see that the photometry is fairly stable for lower wavelengths, but we see higher photometric measurements for some as we get to longer wavelength filters.

We only fit a simple SED with a parametric star formation history (SFH) treatment for our model. We used the redshift (zred) of our source from literature, a Kroupa IMF type, and used Calzetti et al. (2000)'s attenuation curve for the dust around old stars. Lastly, we used a delay-tau form star formation history (sfh=4), where SFR $\sim t_{\rm age} e^{-t_{\rm age}/\tau}$. We have the five free parameters with the following priors: `mass = Uniform(1e8, 1e12)`, metallicity `logzsol = TopHat(-2, 0.19)`, dust attenuation parameter `dust2 = TopHat(0, 2)`, `tage = TopHat(0.001, 13.8)`, and `tau = Uniform(0.1, 30)`. The convergence of these free parameters in our initial, nebular emission free model can be seen in Figure 2.

We then used `PROSPECTOR`'s likelihood and fitting function to vary our free parameters and create an SED

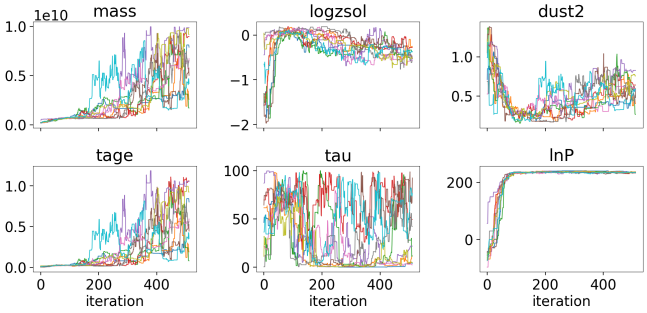

Figure 2. The convergence of parameters for our initial model that does not take into account the nebular emission. In the top row, from left to right, we show the extracted mass, the metallicity, and the dust attenuation model. While in the bottom row, we present the 2 parameters parameters, see Figure 3 for the full posteriors.

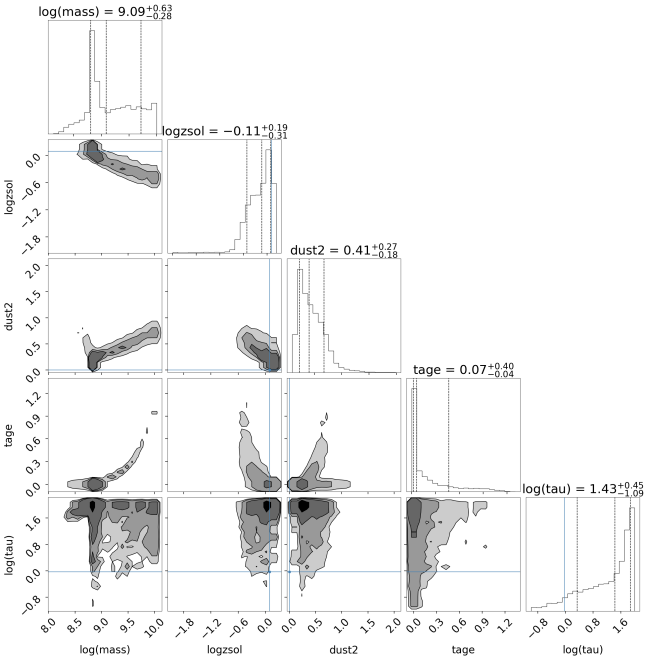

Figure 3. Corner plot showing the best-fit derived galaxy properties. In this iteration of our model, we do not take into account nebular emission. The parameters we extract with this rather simplistic model are star formation history $t_{\rm age} = 0.07^{+0.40}_{-0.04}$ Gyr and $\log(\tau) = 1.43^{+0.45}_{-1.09}$

that best fits the observed measurements we have. This was done with both emcee Foreman-Mackey et al. (2013) and dynesty Speagle (2020). We present our chains for both in Figure 2. We see that the parameters extracted are reasonably burned-in. The posterior distributions for all the parameters we fitted for this initial model can be seen in Figure 3. With this run, we derive the following parameters $M_{\rm gal} = 10^{8.81-9.72}$ $M_\odot$, $Z_{\rm gal} = 10^{-0.42-0.8}$, dust parameter (which is the diffuse dust V-band optical depth) $0.23 - 68$, age of the galaxy

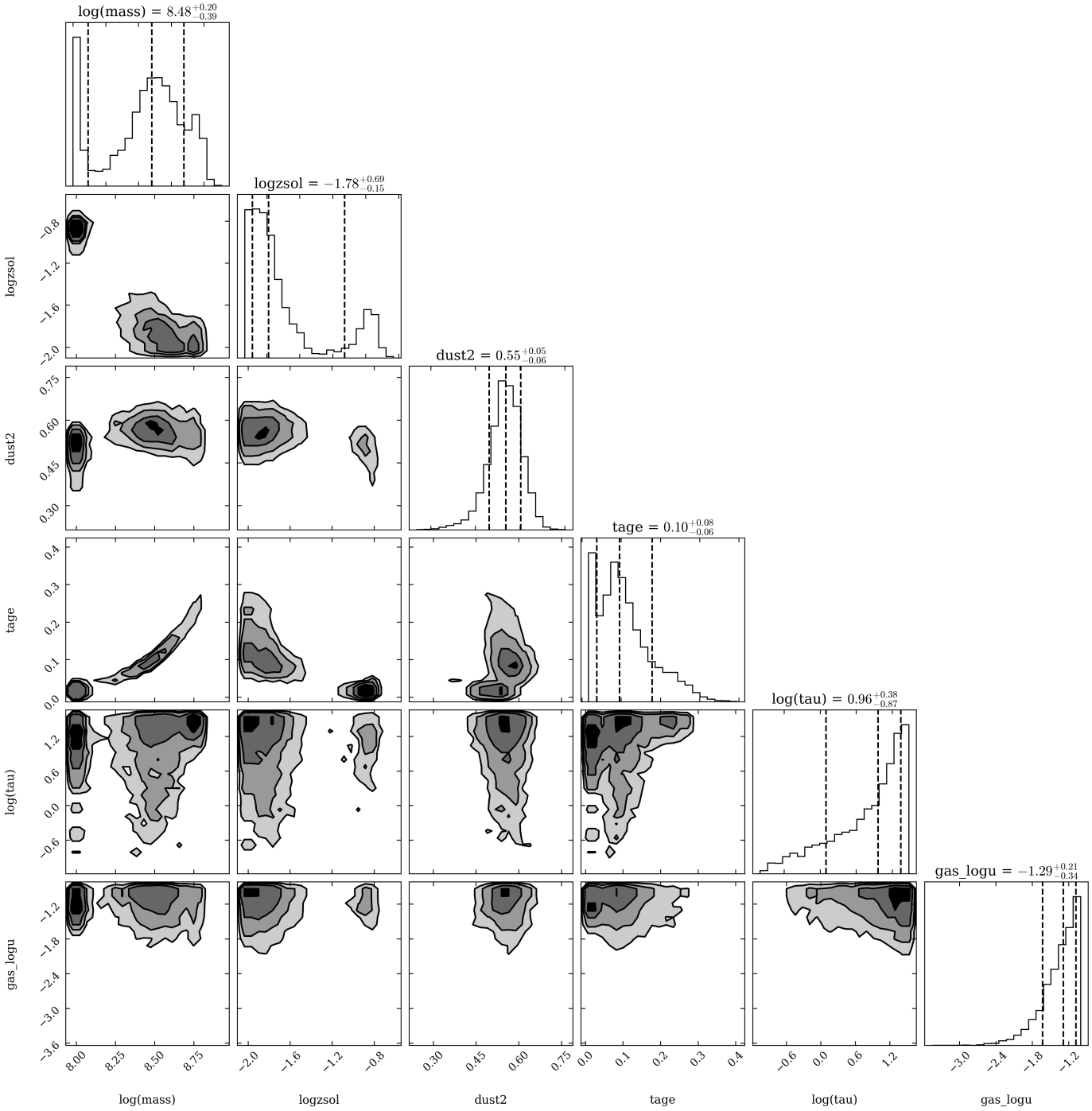

Figure 4. Similar to Figure 3, but including nebular emission from the source. We parametrize this contribution by including fsps's `gas_logu` parameter, which is the gas ionization parameter for the nebular emission model. Note, using fsps also require us to input the metallicity as a parameter into the stellar population model. Notably, having this component reduces stellar mass and metallicity estimates. However it raises slightly dust attenuation and the age of the source. In the end, we find the that the ionization parameter is $-1.29^{+0.21}_{-0.34}$.

$t_{age} \sim 66 - 110$ Myr, and the star formation history parameter $\tau \sim 0.34 - 1.88$.

3.2. *Improvements on the Model*

For our PROSPECTOR model, we can improve its accuracy in describing the observed photometry, by using more realistic parameters and models for our source. Specifically, we can add the nebular continuum coming from the source. This is an important aspect of the model since GS9442 has been shown to exhibit a strong Balmer jump, which can give clues on the nature of the ionizing source. The scenario of a strong nebular emission may imply that either (i) the nebular emission is the dominating source observed, or (ii) the ionizing source that powers such extreme nebular emission outshines the stellar source, which may suggest a top heavy IMF (Cameron et al. 2024). Improved properties of the galaxy can be seen in the posteriors shown in 5. In particular, it brings down the stellar mass estimates as as well as metallicities of the observed galaxy. The dust attenuation is also increased by including nebular emission from the stellar population.

The best model we obtained for our galaxy, along with intermediary steps can be seen in Figure 5. We can see the two models in comparison to the observed photometry in this figure, where the top shows the nebular-emission-free model. We see that including emission from the surrounding gas improves the model slightly. Notably, the Hα + [NII] emission line at $\lambda_{observed} = 6583$ μm and OIII doublet at $\lambda_{observed} \sim 5007$ μm.

4. CONCLUSIONS

To summarize, we used JWST photometry of GS9422 to derive properties of the source. In particular we employed a simple population synthesis code `fsps` to forward-model the photometry assuming with and without nebular continuum. The relevant parameters we derived is the mass of the galaxy, the metallicity, dust attenuation, the age of the object, and the star formation history parameter τ (SFR $\sim t_{age} e^{-t_{age}/\tau}$), and – in the model with nebular emission – the ionization parameter.

1. Using the most basic model we derive that the source has a log mass of $9.09^{+0.63}_{-0.28}$ $M_\odot$, log metallicity of $-0.11^{+0.19}_{-0.31}$ $Z_\odot$, dust attenuation $0.41^{+0.27}_{-0.18}$, galaxy age $0.07^{+0.40}_{-0.04}$ Gyr, and $\tau = 1.43^{+0.45}_{-1.09}$.
2. Including nebular emission, the galaxy properties changes slightly at a log stellar mass of $8.48^{+0.20}_{-0.39}$ $M_\odot$, log metallicity of $-1.78^{+0.69}_{-0.15}$ $Z_\odot$, dust attenuation $0.55^{+0.05}_{-0.06}$, a slightly older age of $0.10^{+0.08}_{-0.06}$ Gyr, $\tau = 0.96^{-0.87}_{+0.38}$, and ionization parameter $-1.29^{+0.21}_{0.34}$.

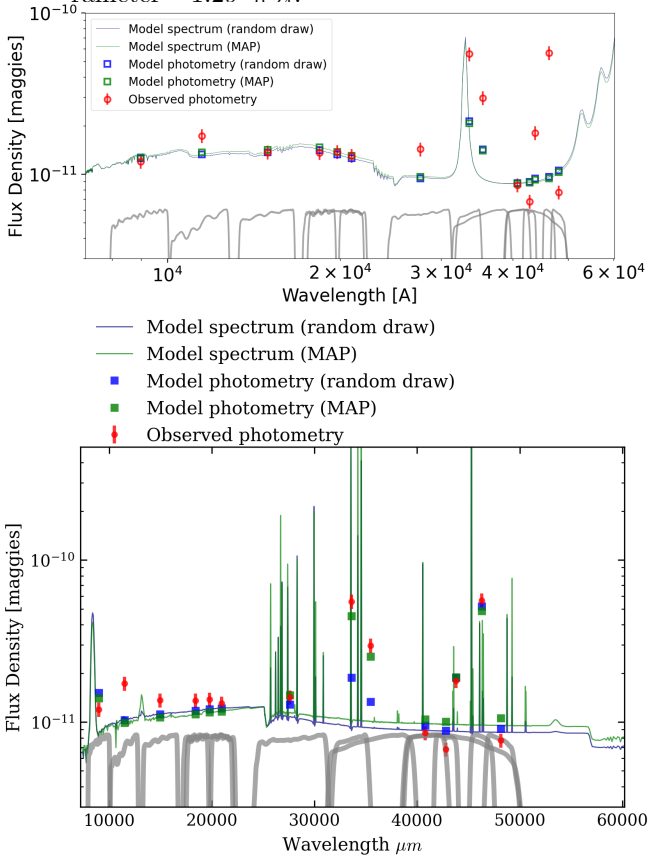

Figure 5. Top panel shows the model spectrum without nebular emission, the the bottom panel shows them with corresponding nebular emission. For a given model spectrum , we have a random draw (before the parameters are inferred by emcee) in blue, the model spectrum found by minimizing the log likelihood in green, and the synthetic photometry corresponding from each by convolving the generated SED.

It is apparent that while including nebular emission qualitatively improves our model, there is still a lot left to be desired. For example, to make our analysis more robust, we can include other SED modelling packages. IN terms of scientific results, the fact that adding nebular emission increases the age of our source, it makes the top-heavy IMF hypothesis put forth by Cameron et al. (2024) less likely, since a star with a mass ~ 100 Myr is rather short-lived, around a few Myr (Kashlinsky 2006)

Software: All the data analysis can be found in this github repository.

REFERENCES

Adamo, A., Atek, H., Bagley, M. B., et al. 2024, arXiv e-prints, arXiv:2405.21054, doi: 10.48550/arXiv.2405.21054

Bunker, A. J., Cameron, A. J., Curtis-Lake, E., et al. 2024, A&A, 690, A288, doi: 10.1051/0004-6361/202347094

Calzetti, D., Armus, L., Bohlin, R. C., et al. 2000, ApJ, 533, 682, doi: 10.1086/308692

Cameron, A. J., Katz, H., Witten, C., et al. 2024, MNRAS, 534, 523, doi: 10.1093/mnras/stae1547

Eisenstein, D. J., Willott, C., Alberts, S., et al. 2023, arXiv e-prints, arXiv:2306.02465, doi: 10.48550/arXiv.2306.02465

Foreman-Mackey, D., Hogg, D. W., Lang, D., & Goodman, J. 2013, PASP, 125, 306, doi: 10.1086/670067

Johnson, B. D., Leja, J., Conroy, C., & Speagle, J. S. 2021, ApJS, 254, 22, doi: 10.3847/1538-4365/abef67

Kashlinsky, A. 2006, New Astronomy Reviews, 50, 208–214, doi: 10.1016/j.newar.2005.11.017

Li, Y., Leja, J., Johnson, B. D., Tacchella, S., & Naidu, R. P. 2024, ApJL, 969, L5, doi: 10.3847/2041-8213/ad5280

Lupi, A., Trinca, A., Volonteri, M., Dotti, M., & Mazzucchelli, C. 2024, A&A, 689, A128, doi: 10.1051/0004-6361/202451249

Rieke, M. J., Robertson, B., Tacchella, S., et al. 2023, ApJS, 269, 16, doi: 10.3847/1538-4365/acf44d

Scholtz, J., Maiolino, R., D'Eugenio, F., et al. 2023, arXiv e-prints, arXiv:2311.18731, doi: 10.48550/arXiv.2311.18731

Speagle, J. S. 2020, MNRAS, 493, 3132, doi: 10.1093/mnras/staa278

Williams, C. C., Tacchella, S., Maseda, M. V., et al. 2023, ApJS, 268, 64, doi: 10.3847/1538-4365/acf130